RSC Advances

PAPER

View Article Online
View Journal | View Issue

Cite this: *RSC Adv.*, 2014, **4**, 8144

A well-defined amphiphilic polymer co-network from precise control of the end-functional groups of linear RAFT polymers

Chao Zhou,[a] Shanshan Qian,[a] Aokai Zhang,[a] Liqun Xu,[b] Jian Zhu,[c] Zhengping Cheng,[c] En-Tang Kang,[b] Fang Yao[a] and Guo Dong Fu*[a]

Received 24th December 2013
Accepted 14th January 2014

DOI: 10.1039/c3ra47939k

www.rsc.org/advances

Linear polystyrene (PS) with well-defined molecular structure and accurate numbers of bromo groups on both ends were synthesized *via* multiple-step alternative RAFT polymerization of *N*-bromopropyl maleimide and β-pinene monomers. The bromo end groups were transformed into the azido moieties *via* nucleophilic substitution. The reaction of as-synthesized linear PS having a named number of azide groups on ends ($(N_3)_x$–PS–$(N_3)_x$) with mono- and dialkynyl-terminated PEG (dA-PEG) *via* copper(I)-catalyzed azide–alkyne cycloaddition (CuAAC) leads to the formation of the well-defined PS–PEG amphiphilic copolymers and polymeric co-networks (APCNs). The as-prepared APCNs exhibit unique ordered separated hydrophilic and hydrophobic phases, and a variable swelling capacity both in polar and non-polar solvents.

Introduction

With a similar porous structure as a bio-membrane that allows small molecules such as cytoplasm and nutrients transport through, hydrogels have potential applications in tissue engineering such as hemodialyzers, artificial skin, and in vascular prostheses.[1,2] As a type of important hydrogels, amphiphilic co-networks (APCNs), composed of covalently interconnected both hydrophilic and hydrophobic segments, exhibit orthogonal chemical and physical properties.[3–6] The hydrophilic and hydrophobic phases would separate at the nano-scale in APCNs when swollen in different polar solvents.[7,8] Due to their unique structures and extraordinary properties, APCNs have found versatile potential applications in soft contact lenses,[9–11] biomaterials for tissue engineering,[12–16] membranes for pervaporation[17] and filtration,[18] catalysis supports,[19–22] and drug carriers.[23–27]

Conventional APCNs, prepared by random free radical copolymerization of multifunctional crosslinkers, are less structure integrity.[28–32] Chemical crosslinking such as Diels–Alder reaction,[33] and Michael-type additions reactions[34–37] between hydrophilic and hydrophobic polymer segments provides an another plausible synthetic approaches for preparing APCNs. However, the low reaction yield and high defects in molecular structure lead to soft, weak and brittle in the APCNs and limit further applications in various fields.

Recently, a kind of APCNs, so-called model APCNs[38–41] has been recently developed by copper(I)-catalyzed azide–alkyne cycloaddition (CuAAC) "Click Chemistry", which has been proved to be a powerful tool for the preparation of polymer network of surprisingly enhanced mechanical properties, well-defined molecular structure and desired functionalities.[42–49] Jérôme[50] and Whittaker[51] prepared biodegradable APCNs by CuAAC. Well-defined poly(ε-caprolactone) (PCL)/poly(ethylene glycol) (PEG) APCNs by CuAAC with excellent biocompatibility and well-controlled drug release were also reported.[52] Reversible addition-fragmentation chain transfer (RAFT) polymerization as one of the most important "Living"/controlled radical polymerization (CRP) techniques,[53–55] has been proved as an effective and convenient tool for the synthesis of polymers with controlled molecular weight and low polydispersity index (PDI) from various monomers.[56–59] The living end group (*e.g.* di- and trithioester) of polymers synthesized *via* RAFT polymerization also can be converted into azide or alkynyl group by substitution reaction.[60–62] Thus, the combination of CuAAC with RAFT polymerization provides a plausible approach to the preparation of APCNs with well-defined molecular structure. However, such a one-to-one group conversion of linear macromolecule is unavailable to the preparation of polymeric networks. Thus, an approach to the synthesis of linear macromolecules with controlled numbers of functional groups at chain ends *via* RAFT polymerization becomes a critical factor to the preparation of well-defined polymer networks *via* the combined CuAAC and RAFT.

In this work, a novel approach was developed for the preparation of linear polystyrene (PS) with accurate number of end groups, *i.e.* bromo, *via* multi-step alternative RAFT chain

[a]*School of Chemistry and Chemical Engineering, Southeast University, Nanjing District, Jiangsu Province, 211189, P.R. China. E-mail: fu7352@seu.edu.cn; Fax: +86-25-52090625; Tel: +86-25-52090625*

[b]*Department of Chemical & Biomolecular Engineering, National University of Singapore, Kent Ridge, 119260, Singapore*

[c]*School of Chemistry, Chemical Engineering and Materials Science, Soochow University, Suzhou, Jiangsu Province, 215123, P.R. China*

extension of *N*-bromopropyl maleimide (PBMI) and β-pinene monomers (Pin). Pin is an electron-rich monomer and PBMI is an electron-deficient monomer. They will not homopolymerize themselves, but will undergo copolymerization with other monomers.[63–65] After removal of trithiocarbonate at the both ends of PS chain, the bromo groups were substituted by azide. The linear PS polymers with accurate number of azido-end groups ($(N_3)_x$–PS–$(N_3)_x$) were subsequently reacted with mone-alkynyl and di-alkynyl terminated poly(ethylene glycol) (dA-PEG) *via* CuAAC to give rise well-defined functional polymer brushes and APCNs.

Experimental section

Materials

Styrene (St, Acros, 99%) was passed through a basic activated aluminum oxide (50–200 microns) column before use. Ethanediol (Shanghai Chemical Reagent, 99%) and propargyl bromide (J&K Scientific, 80%) were dried over distilled under reduced pressure prior to use. Cuprous bromide (CuBr, Acros, 98%) was washed with glacial acetic acid in order to remove any soluble oxidized species. Monomethoxy PEG (M_n = 7600, Alfa Aesar), PEG (M_n = 2000, Aldrich), *N*,*N*,*N*′,*N*′,*N*″-pentamethyldiethylenetriamine (PMDETA, J&K Scientific, 99%), 4-dimethylaminopyridine (DMAP, J&K Scientific, 99%), *N*,*N*′-dicyclohexylcarbodiimide (DCC, Aladdin, 99%), 3-aminopropylbromide hydrobromide (Aladdin, 99%), sodium acetate (Aladdin, anhydrous), maleic anhydride (Aladdin, 99%), β-pinene (Aladdin, 99%) and 1-dodecanethiol (Aladdin, 98%) were used as received.

Synthesis of *N*-bromopropyl maleimide (PBMI)[66]

Triethylamine (10.5 mL, 75.4 mmol) was added dropwise to a mixture of 3-aminopropylbromide hydrobromide (15.0 g, 68.5 mmol) and maleic anhydride (6.72 g, 68.5 mmol) in dichloromethane (200 mL) at 0 °C. After stirring at 25 °C for 2.5 h, the solvent was removed by rotary evaporator, and the residue was extracted by dichloromethane. Then hydrobromic acid (1.25 mL) was added and the mixture was washed with 1 M HBr aqueous solution. The organic phase was dried over magnesium sulfate and filtrated. A white solid was obtained after removal of the solvent by rotary evaporator. The white solid (6.21 g, 26.31 mmol) and sodium acetate (1.10 g, 13.42 mmol) were heated to reflux in acetic anhydride (65 mL) for 23 h. The mixture was poured into 1 M NaOH aqueous solution (600 mL) and the solution was extracted with dichloromethane. The organic phase was dried over magnesium sulfate, filtrated, and evaporated by rotary evaporator. The crude product was purified by silica column chromatography using dichloromethane as the eluent. A white solid (3.02 g, 53%) was obtained. ^{1}H NMR (400 MHz, $CDCl_3$, δ): 2.18 (q, 2H, –CH_2–), 3.37 (t, 2H, –N–CH_2), 3.68 (t, 2H, –CH_2–Br), 6.72 (s, 2H, H═C–).

Synthesis of ethane-1,2-diyl bis(2-(((dodecylthio) carbonothioyl)thio)-2-methylpropanoate) (EDBDCMP)

The bifunctional trithiocarbonate was synthesized as follows: ethylene glycol (0.255 g, 4.11 mmol) was dissolved in 80 mL of dry dichloromethane with 2-(dodecylthiocarbonothiolylthio)-2-methylpropanoic acid (3 g, 8.24 mmol) and catalytic amount of DMAP (0.501 g, 4.11 mmol). After the solution was homogenized by stirring for 10 min, DCC (3.39 g, 16.48 mmol) in dry dichloromethane (10 mL) was added dropwise. The solution was stirred at 25 °C for 24 h. The organic phase was successively washed with 1 M HCl solution and 5% sodium hydroxide solution and saturated sodium chloride solution thrice (3 × 100 mL). After drying over magnesium sulfate for 24 h, the solution was concentrated and purified by silica column chromatography using hexane and dichloromethane (v/v = 1 : 1) as the eluent, giving rise to a yellow oil. (Yield = 51%) ^{1}H NMR (400 MHz, $CDCl_3$, δ): 4.31 (s, 4H, –O–CH_2), 1.70 (s, 12H, –C–$(CH_3)_2$), 3.28 (t, 4H, –CH_2–S–), 1.27 (m, 36H, –$(CH_2)_{10}$–), 0.90 (t, 6H, –CH_3).

Synthesis of alkynyl terminated PEG[67]

Monomethoxy PEG (M_n = 7600) (7.60 g, 1 mmol) was dissolved in dry tetrahydrofuran (THF) (30 mL) in three-necked 250 mL round-bottom flask, equipped with magnetic stirrer, thermometer and reflux condenser at 0 °C. NaH (0.432 g, 18 mmol) was added to the solution under nitrogen atmosphere. After stirring for 1 h, propargyl bromide (0.30 mL, 3.9 mmol) was added dropwise into the solution. The mixture was stirred for 30 min at 0 °C and then stirred for another 24 h at room temperature. Then, the reaction mixture was filtered, and evaporated under reduced pressure to produce the product. (4.90 g, Yield = 92%). ^{1}H NMR (400 MHz, $CDCl_3$, δ): 4.21 (d, 2H, CH_2–C), 3.65–3.56 (m, 430H, –CH_2–O–), 3.39 (t, 3H, CH_3–O–), 2.40 (t, 1H,–C–CH). The di-alkynyl terminated PEG (M_n = 2000) was synthesized similar to alkynyl terminated monomethoxy PEG. ^{1}H NMR (400 MHz, $CDCl_3$, δ): 4.21 (d, 4H, CH_2–C), 3.65–3.56 (m, 196H, –CH_2–O–), 2.40 (t, 2H, –C–CH).

Synthesis of linear PS by RAFT polymerization

A mixture of EDBDCMP (0.1093 g, 0.145 mmol), styrene (4.53 g, 43.5 mmol), and AIBN (4.76 mg, 0.029 mmol) were charged in a 10 mL round-bottom flask. The reaction mixture was degassed by performing three successive freeze–pump–thaw cycles, sealed and then put into a pre-heated oil bath at 60 °C for 9 h under nitrogen atmosphere. After reaction, the resultant mixture was dissolved in THF and precipitated into an excess amount of methanol for three times and dried in vacuum at room temperature overnight. The linear PS was obtained with yield of 20%.

Synthesis of Br–PS–Br by RAFT

The prepared linear PS was used as macro RAFT agent (PS CTA) (0.67 g, 0.15 mmol) and was dissolved in 2 mL toluene with PBMI (0.327 g, 1.5 mmol), AIBN (2.4 mg, 0.015 mmol). Then, the reaction mixture was degassed by performing three successive freeze–pump–thaw cycles, and was sealed and then put into a pre-heated oil bath at 60 °C for 24 h under nitrogen atmosphere. After predetermined time, the resultant mixture was dissolved in THF and precipitated into an excess amount of methanol for

three times and dried in vacuum at room temperature overnight.

Synthesis of PinBr–PS–BrPin by RAFT

The prepared Br–PS–Br (0.5 g, 0.09 mmol), β-pinene (0.123 g, 0.9 mmol), AIBN (1.37 mg, 0.009 mmol) were dissolved in 2 mL 1,2-dichloroethane and degassed by performing three successive freeze–pump–thaw cycles. The reaction mixture was sealed and then put into a pre-heated oil bath at 60 °C for 24 h under nitrogen atmosphere. After predetermined time, the resultant mixture was dissolved in THF and precipitated into an excess amount of methanol for three times and dried in vacuum at room temperature overnight.

The copolymerization procession of $(Br)_2$–PS–$(Br)_2$, PinBr-PinBr–PS–BrPinBrPin and $(Br)_3$–PS–$(Br)_3$ were similar to step 2 and 3.

Removal of trithiocarbonate groups and synthesis of $(N_3)_x$–PS–$(N_3)_x$ ($x = 1, 2, 3$) polymers

A mixture of prepared $(Br)_x$–PS–$(Br)_x$ ($x = 1, 2, 3$) (0.067 mmol), AIBN (4.02 mmol) and toluene (5.0 mL) was added in an ampoule and was heated to 60 °C under nitrogen atmosphere for 12 h. The solution was precipitated into methanol, giving white powder.

Sodium azide (1.1 equiv.) and as prepared polymers (1 equiv.) were dissolved in *N*,*N*-dimethyl formamide (DMF). The reaction mixture was stirred at room temperature for 12 h. Afterward, the reaction mixture was diluted with CH_2Cl_2 and washed with water for thrice. The organic phase was evaporated in vacuum and precipitated into excess methanol. $(N_3)_x$–PS–$(N_3)_x$ ($x = 1, 2, 3$) were obtained after dried in vacuum at room temperature overnight.

Click chemistry of $(N_3)_x$–PS–$(N_3)_x$ ($x = 1, 2, 3$) and mono-alkynyl terminated PEG

N_3–PS–N_3, $(N_3)_2$–PS–$(N_3)_2$, $(N_3)_3$–PS–$(N_3)_3$ and mono-alkynyl terminated PEG ($M_n = 7600$) (1 : 2.1, 1 : 4.1 and 1 : 6.1) were dissolved in 2 mL of DMF in a nitrogen-purged flask, respectively. Then CuBr and PMDETA were added under a nitrogen environment and stirred at 30 °C for 24 h. After this specified time, the polymer solution was diluted in dichloromethane and passed through basic alumina column to remove copper salt. Next, the mixture was evaporated in vacuum and the residue dissolved in methanol, and poured into dialysis bag, dialyzed in deionized water for 48 h. Finally, the polymer solution in dialysis bag was evaporated, and dried in vacuum at room temperature overnight.

Preparation of PS–PEG APCNs *via* Click Chemistry

$(N_3)_2$–PS–$(N_3)_2$ (20 mg, 0.0033 mmol), di-alkyne terminated PEG ($M_n = 2000$) (13.3 mg, 0.0066 mmol), PMDETA (1.36 μL, 0.0066 mmol) and DMF 1 mL were introduced into a small vial. After the mixture turned clear, the vial was degassed with nitrogen for 20 min, 0.94 mg (0.0066 mmol) of CuBr was quickly added under ultrasonic agitation. Gelation of the APCN was obtained in about 1 min. After keeping at room temperature for 24 h, a uniform APCN were obtained. The gels were transferred to an EDTA (5%) solution to remove the copper ions and DMF. Finally, the gels were immersed into a large volume of deionized water to allow full water absorption. The other gel from $(N_3)_3$–PS–$(N_3)_3$ was also prepared in the same way in 1 mL DMF at room temperature. (Molar ratio: [$(N_3)_3$–PS–$(N_3)_3$] : [dA-PEG] : [CuBr] : [PMDETA] = 1 : 3 : 3 : 3).

Characterization

^{1}H NMR spectra were obtained on AVANCE 400 MHz spectrometer (Bruker), using the solvent signal for calibration. IR spectra were obtained using a 670-IR FT-IR spectrometer (Varian Company). UV-vis spectra were recorded on a UV-1750 UV-vis spectrometer (Shimadzu) in the wavelength range from 250 to 600 nm. Measurements were carried out in solution (THF). Gel permeation chromatography (GPC) was carried out on a Waters model 1515 series pump (Milford, MA) with Waters Styragel column (HR 5E), (4.6 mm internal diameter, 300 mm length, packed with 5 μm particles) were used. The system was fitted with a Model 2414 differential refractometer detector and anhydrous tetrahydrofuran was used as the mobile phase (1 mL min^{-1} flow rate). The calculated molecular weight was based on calibration using linear polystyrene standards. Data was collected and analyzed using Breeze software was conducted to measure molecular weights in THF with a flow rate of 1 mL min^{-1} at 40 °C. PS standards were used as the references. Typical sample concentrations for GPC analysis were in the range of 3 mg mL^{-1} depending on molecular weight and filtered through 0.22 μm pore size PA membrane filter. Injection volume of the sample solutions were 20 μL. XPS measurements were carried out on a Kratos AXIS HSi spectrometer (Kratos Analytical Ltd.) with a monochromatized Al KR X-ray source (1486.6 eV photons). The X-ray source was run at a reduced power of 150 W (15 kV and 10 mA). The samples were mounted on the standard sample studs by means of double-sided adhesive tapes. The core-level spectra were obtained at the photoelectron takeoff angle (with respect to the sample surface) of 90°. The pressure in the analysis chamber was maintained at 10–8 Torr or lower during sample measurements. The morphology of the APCNs was studied on a JSM-6510 scanning electron microscope (SEM) (JEOL) at an accelerating voltage of 30 kV. The swollen gels were dried in a FD-1A-50 (Bilon Co.) freeze-dryer. Differential scanning calorimetry (DSC) measurement was conducted on a TA Instrument DSC Q-10 over the temperature range from −45 to 135 °C at a heating rate of 10 °C min^{-1} under nitrogen environment. DSC was calibrated with metallic indium (99.9% purity). The thermal stability of the prepared network, were carried out on a SDT-Q600 thermogravimetric analyzer (TA Instruments) at a temperature ranging from 50 to 800 °C at heating rate of 10 °C min^{-1} under nitrogen atmosphere. Swelling behavior of the prepared PS–PEG networks was measured by a gravimetric method. Dry gels were immersed in THF, methanol and water respectively at 25 °C, and the samples were taken out at certain time intervals, wiped

by a filter paper, and weighed. Swelling ratio (SR) of PS–PEG networks were determined gravimetrically using the following eqn (1):

$$SR = (m_t - m_0)/m_0 \times 100\% \quad (1)$$

here m_t is the mass of the swollen network at time t and m_0 is the mass of the dry gel.

Result and discussion

The synthesis of PS with named number of azide groups on ends ($(N_3)_x$–PS–$(N_3)_x$, $x = 1, 2, 3$) is the key for preparation of well-defined amphiphilic co-network *via* combined RAFT and CuAAC. The synthesis of $(N_3)_x$–PS–$(N_3)_x$ ($x = 1, 2, 3$) is shown in Scheme 1. Initially, linear α,ω-trithiocarbonate end-functionalized PS was prepared *via* RAFT polymerization using ethane-1,2-diyl bis(2-(((dodecylthio)carbonothioyl)thio)-2-methylpropanoate) (EDBDCMP) as the chain transfer agent (CTA). β-Pinene (Pin) is an electron-rich monomer and *N*-bromopropyl maleimide (PBMI) is an election-deficient monomer. Thus, they will not homopolymerize themselves, but will undergo copolymerization with each other. Linear PS polymers with exactly 2, 4 or 6 bromo groups on both ends ($(Br)_x$–PS–$(Br)_x$, $x = 1, 2, 3$) were obtained after a predetermined steps of alternative RAFT polymerization of PBMI and Pin (Scheme 1). After removal of the butyl trithiocarbonate (BTTC) groups, bromo groups on PS chain ends were transformed into azide groups by a substitution reaction with sodium azide. Subsequent CuAAC reaction of $(N_3)_x$–PS–$(N_3)_x$ ($(N_3)_x$–PS–$(N_3)_x$, $x = 2, 3$) with dA-PEG produced the well-defined PS–PEG co-networks (APCNs) (Fig. 1).

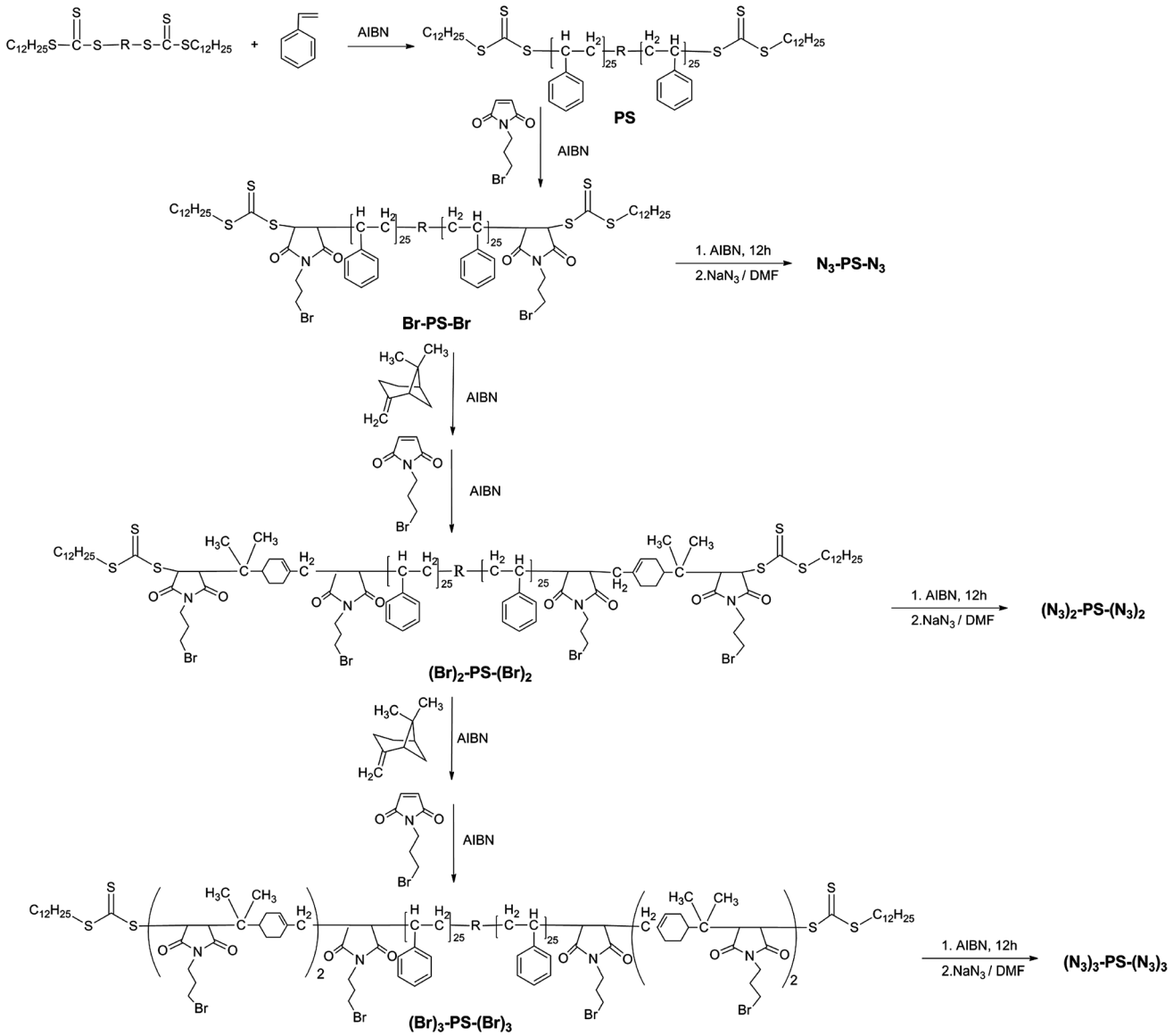

Scheme 1 Schematic illustration of the synthesis of $(Br)_x$–PS_{50}–$(Br)_x$ ($x = 1, 2, 3$) copolymers with *N*-bromopropyl maleimide (PBMI) and β-pinene (Pin) by multi-step RAFT polymerization and the synthesis of $(N_3)_x$–PS_{50}–$(N_3)_x$ ($x = 1, 2, 3$) by nucleophilic substitution.

Polymer synthesis

Initial polymerization of linear PS (PS CTA) using bifunctional EDBDCMP was found to proceed reasonably, with 20% conversion to give M_n of 4.6×10^3 g mol^{-1} and PDI of 1.09 after 9 h (Fig. 2A). The degree of polymerization (DP) of PS is about 44 based on GPC result. The successful preparation of PS can also be characterized with a ^{1}H NMR spectrum (Fig. 3(a)). The DP of prepared PS CTA can be calculated from the ratio of integral area of the methylene protons at the ω chain end at 1.26 ppm and the aromatic protons in the range of 6.3–7.2 ppm. The DP of PS macro-CTA is about 50, which is very close to the GPC results.

Subsequent RAFT chain extension of PBMI monomer from PS CTA gave rise to the Br–PS_{50}–Br polymer. The new chemical shifts appeared at 3.68 and 3.36 ppm, assigned to the methylene protons (m, k) near the amide bounds in Br–PS_{50}–Br suggest that the PBMIs were successfully introduced on the PS chain ends (Fig. 3(b)). The M_n of Br–PS_{50}–Br remained at 5.4×10^3 g mol^{-1} even when the polymerization time was increased from 24 h to 48 h, suggesting non-homopolymerization of PBMI. The ^{1}H NMR results indicate that there are about 1.96 Br groups at the Br–PS_{50}–Br chain ends. In another word, only one PBMI was introduced on to the macromolecules at each CTA site with one step of RAFT polymerization of PBMI.

XPS analysis was also carried out to verify the successful preparation of the Br–PS_{50}–Br. Fig. 4(a) and (c) show the XPS wide-scan spectrum of PS_{50} and Br–PS_{50}–Br copolymer. In comparison to the XPS wide-scan spectrum of PS_{50} CTA, the appearance of the Br 3d signal at the binding energy (BE) of 68.4 eV and N 1s signal at the BE of 400.0 eV are consistent with the appearance of PBMI on PS_{50} chains. The C 1s core-level spectrum of Br–PS_{50}–Br (Fig. 4(b)) can be curve-fitted into four peak components with BE's at about 284.9 eV, 286.2 eV, 286.8 eV and 291.3 eV, attributable to the *C*–C/C–H, *C*–O/*C*–S, *C*=O and π–π* shakeup satellite transition, respectively.[68] The new peak components appeared at BE's of about 289.2 and 285.6 eV attributable to the O=*C*–N- and *C*–N/*C*–Br species[69] indicate the successful preparation of Br–PS_{50}–Br (Fig. 4(d)). The [*C*–N]/[*C*–Br] : [O=*C*–N] : [*C*=O] peak components area ratio of about 1.0 : 1.1 : 0.6 is consistent with the theoretical value ([*C*–N]/[*C*–Br] : [O=*C*–N] : [*C*=O] ratio of 1.0 : 1.0 : 0.5), suggesting that the successful preparation of Br–PS_{50}–Br copolymer.

The synthesis of PinBr–PS_{50}–BrPin was carried out by another step of RAFT chain extension from Br–PS_{50}–Br macro-CTA using Pin as the monomer. Fig. 3(c) shows the ^{1}H NMR result of PinBr–PS_{50}–BrPin. The new peaks in the range of δ 5.18 ppm is attributable to the endo-olefin (o) protons and that at δ 2.33 assigned to the methylene (p) protons.[70] While, the chemical shifts of PBMI appeared as a broad signal at 3.36 and 3.68 ppm due to the adjacent Pin units. The number of the Pin groups can also be calculated from the integrated peak area ratio of protons at δ 2.33 and 3.36 ppm. About 1.90 Pin end groups were introduced on the polymer chain. The non-homopolymerization of Pin was also revealed by the fact that the M_n of PinBr–PS_{50}–BrPin was remained unchanged with the extension polymerization time from 24 to 48 hours. The Pin radical has considerable reactivity toward PBMI, because PBMI is an electron-deficient radical whose addition to the electron-rich Pin is facilitated by the possible charge-transfer complexation in the transition state.[71]

$(Br)_2$–PS_{50}–$(Br)_2$ was prepared by RAFT chain extension of PinBr–PS_{50}–BrPin macro-CTA and PBMI monomers. In Fig. 3(d), the sharp peaks appeared at 3.36 and 3.68 ppm and the broad of the endo-olefin signals at 5.1–5.25 ppm of β-pinene (Pin) units due to the effect of the adjacent *N*-substituted maleimide units suggest the preparation of the $(Br)_2$–PS_{50}–$(Br)_2$.[72] PinBrPinBr–PS_{50}–BrPinBrPin and $(Br)_3$–PS_{50}–$(Br)_3$ were synthesized by another step RAFT polymerization. Table 1 shows the content of the end functional groups of $(Br)_x$–PS_{50}–$(Br)_x$ (x = 1, 2, 3) copolymers calculated from ^{1}H NMR results. The number, *i.e.* 1.96, 3.74 and 5.39, of Br groups on Br–PS_{50}–Br, $(Br)_2$–PS_{50}–$(Br)_2$, $(Br)_3$–PS_{50}–$(Br)_3$ copolymers are very close to the respective theoretical values of 2, 4 and 6. It was also qualitatively confirmed in FT-IR spectra (Fig. 5) by the enhancement of peak at 1720 cm^{-1} assigned to C=O in the cyclic anhydride group of

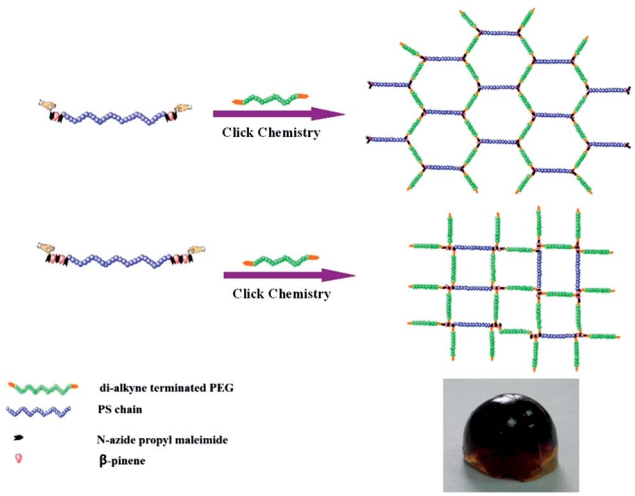

Fig. 1 Illustration of end groups tailing at PS chain ends, and the preparation of $APCN_{PS_{50}\text{-}(PEG45)_2}$ and $APCN_{PS_{50}\text{-}(PEG45)_3}$ with di-alkynyl terminated poly(ethylene glycol) (dA-PEG, M_n = 2000) by "Click Chemistry", and the photograph of $APCN_{PS_{50}\text{-}(PEG45)_3}$.

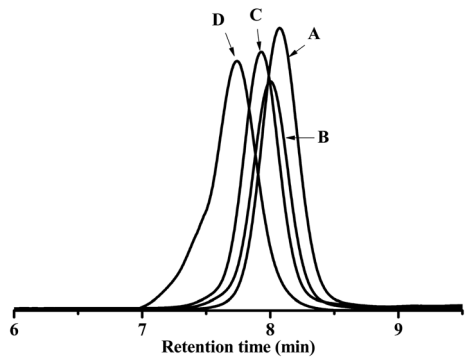

Fig. 2 Gel Permeation Chromatography (GPC) curves of (A) PS_{50} CTA, (B) Br–PS_{50}–Br, (C) $(Br)_2$–PS_{50}–$(Br)_2$ and (D) $(Br)_3$–PS_{50}–$(Br)_3$ copolymers by multi-step RAFT polymerization (eluent: tetrahydrofuran (THF), 40 °C, PS standards).

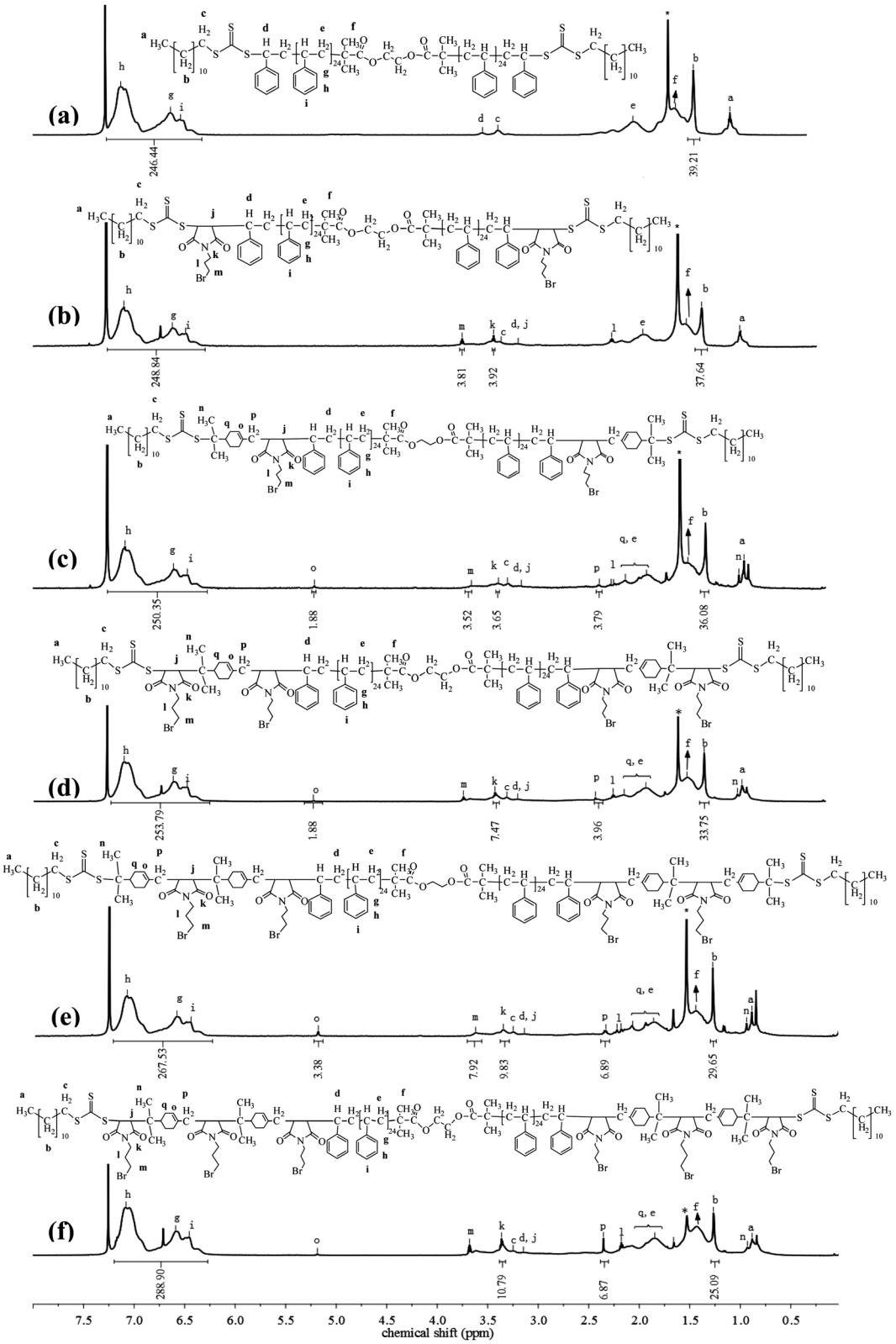

Fig. 3 ^{1}H NMR ($CDCl_3$, 400 MHz) of (a) PS_{50} CTA, (b) Br–PS_{50}–Br, (c) PinBr–PS_{50}–BrPin, (d) $(Br)_2$–PS_{50}–$(Br)_2$, (e) BrPinBr–PS_{50}–BrPinBr and (f) $(Br)_3$–PS_{50}–$(Br)_3$ by RAFT (in Table 1). Pin = β-pinene.

PBMI after multi-step RAFT polymerization. Furthermore, the increase in the ratio of [Br] : [C] from 0.015 to 0.032 is consist with the successful preparation of $(Br)_x$–PS_{50}–$(Br)_x$ (Table 2). The area ratio of [*C*–N]/[*C*–Br] : [O=*C*–NH] : [*C*=O] peak components of $(Br)_x$–PS_{50}–$(Br)_x$ (x = 1, 2, 3) in XPS C 1s core-level spectrum are 2.2 : 2.3 : 1.2, 4.8 : 4.9 : 1.3, 9.8 : 9.1 : 1.3,

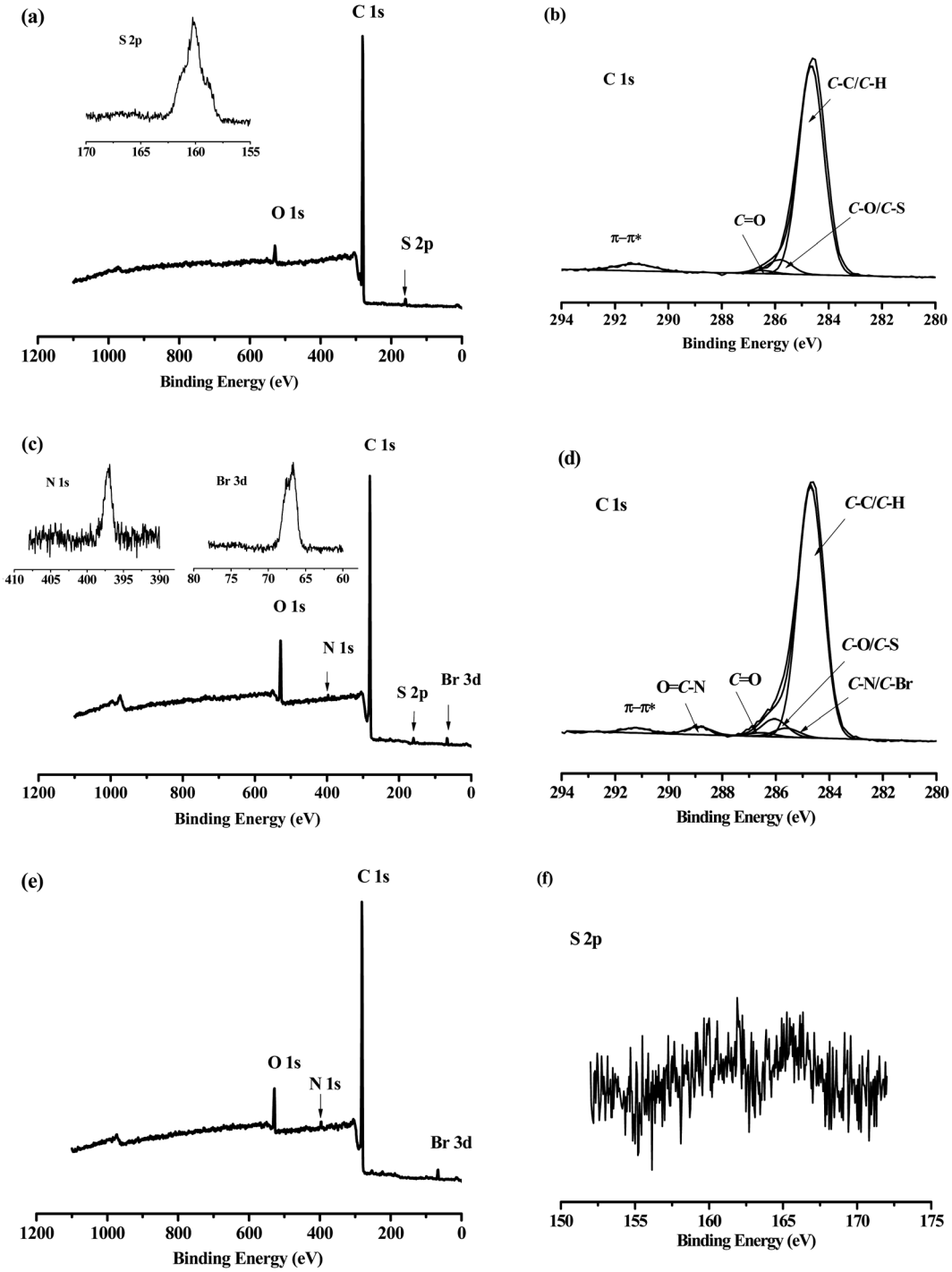

Fig. 4 X-ray photoelectron spectra (XPS) wide-scan of (a) PS_{50} CTA, (c) Br–PS_{50}–Br by RAFT, (e) trithioester end group removed of Br–PS_{50}–Br, and XPS C 1s core-level spectra of (b) PS_{50} CTA, (d) Br–PS_{50}–Br, and (f) XPS S 2p core-level spectra of Br–PS_{50}–Br after removal of trithioester end group.

which are close to their theoretical value 2.0 : 2.0 : 1.0, 4.0 : 4.0 : 1.0, and 8.0 : 8.0 : 1.0, respectively. In Fig. 2, GPC curve traces shows that the M_n increase from 5.4×10^3 to 7.4×10^3, which indicates the successful preparation of $(Br)_x$–PS_{50}–$(Br)_x$ ($x = 1, 2, 3$).

The inactivation of BTTC groups in multiple step RAFT chain extension is the main concern in this work. Previous work suggests a slow addition-fragmentation process in the copolymerization at a low monomer concentration would result in the losing of the trithiol end group in RAFT polymerization.[73–75] Thus, in order to inhibit the inactivation of the BTTC in the multiple-step of RAFT, the feed ratio [M]/[macro-CTA] = 10 : 1 was adopted. The PDIs of $(Br)_x$–PS_{50}–$(Br)_x$ ($x = 1, 2, 3$) copolymer increase from 1.09 to 1.12 and 1.20, which may account for part

Table 1 Characteristics of polymers

Polymer structure	[St] : [PBMI] : [Pin] Theory[a]	[St] : [PBMI] : [Pin] ^{1}H NMR[b]	Number of azide groups in a macromolecule	Number of PEG brushes in macromolecule	Concentration of butyl trithiocarbonate[e] (%)	GPC results M_n (kg mol^{-1})	GPC results M_w (kg mol^{-1})	GPC results PDI
PS_{50}	50 : 0 : 0	50 : 0 : 0	—	—	—	4.6	5.0	1.09
Br–PS_{50}–Br	50 : 2 : 0	50 : 1.96 : 0	—	—	96.6	5.4	5.8	1.09
PinBr–PS_{50}–BrPin	50 : 2 : 2	50 : 1.96 : 1.90	—	—	93.4	5.6	6.1	1.10
$(Br)_2$–PS_{50}–$(Br)_2$	50 : 4 : 2	50 : 3.74 : 1.90	—	—	91.7	6.1	6.8	1.12
PinBrPinBr–PS_{50}–BrPinBrPin	50 : 4 : 4	50 : 3.74 : 3.45	—	—	85.1	6.7	7.7	1.15
$(Br)_3$–PS_{50}–$(Br)_3$	50 : 6 : 4	50 : 5.39 : 3.45	—	—	82.9	7.4	8.8	1.20
N_3–PS_{50}–N_3	—	—	2.0[c]	—	—	5.2	6.3	1.20
$(N_3)_2$–PS_{50}–$(N_3)_2$	—	—	3.57[c]	—	—	5.7	6.8	1.21
$(N_3)_3$–PS_{50}–$(N_3)_3$	—	—	6.23[c]	—	—	7.0	8.6	1.23
Mono-alkynyl terminated PEG_{173}	—	—	—	—	—	7.6	7.9	1.03
PEG_{173}–PS_{50}–PEG_{173}	—	—	—	2.3[d]	—	22.6	27.1	1.20
$(PEG_{173})_2$–PS_{50}–$(PEG_{173})_2$	—	—	—	4.2[d]	—	37.5	44.9	1.20
$(PEG_{173})_3$–PS_{50}–$(PEG_{173})_3$	—	—	—	6.3[d]	—	54.8	71.2	1.30

[a] The theoretic values assume the conversion is 100% in each step. [b] Calculated from the integrated area ratio of ^{1}H NMR spectrum. [c] Calculated from area ratio of integrated signals at 2090 cm^{-1} assigned to azide and at 757 cm^{-1} to phenyl group (FT-IR results). [d] Calculated from the eqn (3). [e] The value was determined from absorbance at λ_{max} = 320 nm of the UV-vis spectrum.

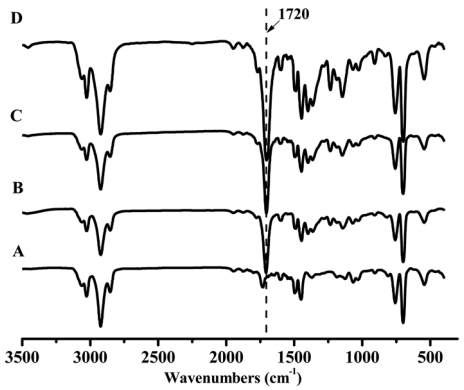

Fig. 5 FT-IR spectra of (A) PS_{50} CTA, (B) Br–PS_{50}–Br, (C) $(Br)_2$–PS_{50}–$(Br)_2$ and (D) $(Br)_3$–PS_{50}–$(Br)_3$ copolymers (1720 cm^{-1}).

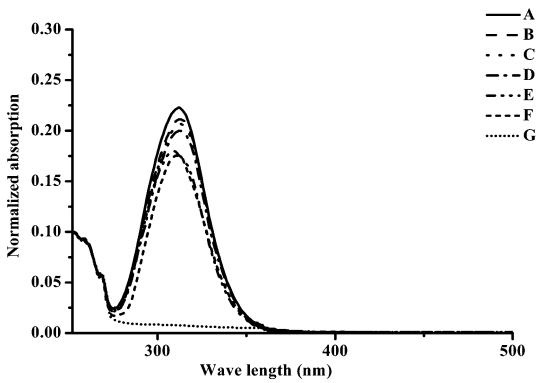

Fig. 6 UV-vis absorption curves of (A) PS_{50} CTA, (B) Br–PS_{50}–Br, (C) PinBr–PS_{50}–BrPin, (D) $(Br)_2$–PS_{50}–$(Br)_2$, (E) PinBrPinBr–PS_{50}–BrPinBrPin, (F) $(Br)_3$–PS_{50}–$(Br)_3$, and (G) Br–PS_{50}–Br after removal of BTTC groups on ends. BTTC = butyl trithiocarbonate.

Table 2 XPS aromatic characteristics of polymers

Polymer structure	[N]/[C]	[Br]/[C]	[S]/[C]
PS_{50}	—	—	0.044
Br–PS_{50}–Br	0.028	0.015	0.023
$(Br)_2$–PS_{50}–$(Br)_2$	0.047	0.024	0.011
$(Br)_3$–PS_{50}–$(Br)_3$	0.057	0.032	0.008
N_3–PS_{50}–N_3	0.116	—	—
$(N_3)_2$–PS_{50}–$(N_3)_2$	0.132	—	—
$(N_3)_3$–PS_{50}–$(N_3)_3$	0.153	—	—

losing of BTTC groups. Fig. 6 shows the UV-vis absorption spectrum of trithiocarbonate. The trithiocarbonate groups has a maximum absorption at λ_{max} = 320 nm, and its intensity decreases with the increase in RAFT polymerization steps. The percentage of the trithiocarbonate in various chain extension polymers can be calculated according to eqn (2):

$$\text{Percentage}_{(\text{UV-vis})} = 1 - (\text{Abs}_{320(o)} - \text{Abs}_{320(t)})/\text{Abs}_{320(o)} \quad (2)$$

where $\text{Abs}_{320(t)}$ is the absorbance of $(Br)_x$–PS_{50}–$(Br)_x$ (x = 1, 2, 3), $\text{Abs}_{320(o)}$ is the trithiocarbonate absorbance of PS CTA. The concentration of trithiocarbonate in Br–PS_{50}–Br shown in Table 1 is about 96.6%, while for $(Br)_2$–PS_{50}–$(Br)_2$ and $(Br)_3$–PS_{50}–$(Br)_3$, the value decreases to 91.7% and 82.9%, respectively. Chemical composition analysis by XPS (Table 2) also shows that the [S]/[C] ratio in Br–PS_{50}–Br is 0.023, while it decreases to 0.011 in $(Br)_2$–PS_{50}–$(Br)_2$ and to 0.008 in $(Br)_3$–PS_{50}–$(Br)_3$ copolymers. The

reduction in [S]/[C] is attributable to the increase of carbon atoms and inactivation of BTTC groups.

Synthesis of $(N_3)_x$–PS_{50}–$(N_3)_x$

To avoid the side reaction,[76] the trithioester end group were removed by large amount of AIBN initiation before the substitution reaction. The successful removal of trithiocarbonate groups at the ends of Br–PS_{50}–Br was confirmed by the disappearance of absorbance at $\lambda_{max} = 320$ nm of UV-vis spectrum in Fig. 6. Fig. 4(e) and (f) shows the XPS wide-scan S 2p core-level spectrum of Br–PS_{50}–Br after removal of RAFT groups, respectively. In comparison to Br–PS_{50}–Br (Fig. 4(c)), the disappearance of S 2p signal at BE's 160.1 eV indicates the successful removal of the trithiocarbonate groups.

NaN_3 nucleophilic substitution was performed after removal of trithiocarbonate groups at the ends of $(Br)_x$–PS_{50}–$(Br)_x$. In the FT-IR spectrum (Fig. 7), the strong absorbance representing the valence vibration of azide groups was observed at 2090 cm^{-1},[77] confirmed the successful preparation of $(N_3)_x$–PS_{50}–$(N_3)_x$ ($x = 1$, 2, 3). The number of azide groups in a $(N_3)_x$–PS_{50}–$(N_3)_x$ molecule can be calculated from the increase integrated peak area at 2090 cm^{-1} in comparison to that at 757 cm^{-1}, which assigned to the asymmetrical stretch of azide group and C–H bending of benzenyl group, respectively. The number of azide groups in N_3–PS_{50}–N_3, $(N_3)_2$–PS_{50}–$(N_3)_2$ and $(N_3)_3$–PS_{50}–$(N_3)_3$ is 2.0, 3.57 and 6.32 according to the FT-IR results (Table 1). In Fig. 8(a), the disappearance of the Br 3d signal at the BE of 68.4 eV and the stronger N 1s signal at the BE of 400.0 eV are consistent with the successful preparation of N_3–PS_{50}–N_3. The number of azide groups on $(N_3)_x$–PS_{50}–$(N_3)_x$ can also determined from the XPS results. Fig. 8(b) shows the XPS N1s core-level spectrum of N_3–PS_{50}–N_3 polymers. The spectrum was curve-fit into four peaks, at BE's of 401.1 eV assigned to O═C–*N*–C═O, at 398.8 eV assigned to C*N*, at 400.0 eV account to $N^- = N^+ = N^-$, and at 403.8 eV s assigned $N^- = N^+ = N^-$, respectively.[78] The number of azide on N_3–PS_{50}–N_3 can be calculated from the peak area ratio at BE's of [O═C–*N*–C═O] : [$N^- = N^+ = N^-$] : [C*N*] = 19.7 : 19.5 : 20.6, which in accordance with their theoretical value 1.0 : 1.0 : 1.0. That is identified there are 2 azide groups in a N_3–PS_{50}–N_3, which is close to the FT-IR and NMR results. The area ratio of [O═C–*N*–C═O] : [$N^- = N^+ = N^-$] : [C*N*] in $(N_3)_2$–PS_{50}–$(N_3)_2$ and $(N_3)_3$–PS_{50}–$(N_3)_3$ are 21.3 : 22.4 : 12.9, 22.7 : 23.3 : 8.2, respectively, which are very close to the theoretical ratio of 2.0 : 2.0 : 1.0, 3.0 : 3.0 : 1.0.

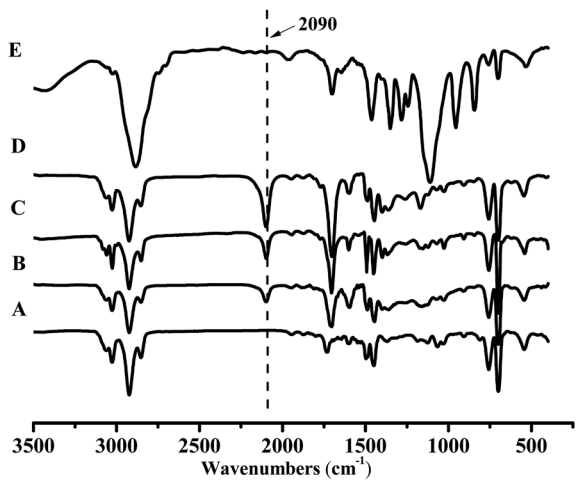

Fig. 7 FT-IR spectra of (A) PS_{50} CTA, (B) N_3–PS_{50}–N_3, (C) $(N_3)_2$–PS_{50}–$(N_3)_2$, (D) $(N_3)_3$–PS_{50}–$(N_3)_3$ polymers, verifying the increase of the azide (2090 cm^{-1}) and (E) $(PEG_{173})_2$–PS_{50}–$(PEG_{173})_2$ polymer brush from "Click Chemistry" by $(N_3)_2$–PS_{50}–$(N_3)_2$ and mono-alkynyl terminated PEG_{173} ($M_n = 7600$).

Synthesis of $(PEG)_x$–PS_{50}–$(PEG)_x$ copolymers

Well-defined $(PEG)_x$–PS_{50}–$(PEG)_x$ amphiphilic block polymers were prepared to further determine the content of azide groups in $(N_3)_x$–PS_{50}–$(N_3)_x$. Click reactions of $(N_3)_x$–PS_{50}–$(N_3)_x$ and mono-alkynyl terminated PEG with a M_n of 7.6×10^3 g mol^{-1} (PDI = 1.03) (PEG_{173}) was carried out using CuBr/PMDETA as the catalyst in DMF at 30 °C for 24 h. Fig. 7 shows the FT-IR results of a $(PEG_{173})_2$–PS_{50}–$(PEG_{173})_2$ amphiphilic block polymers. The complete disappearance of peak signal at 2090 cm^{-1} accounting for azide vibration reveals the complete of CuAAC. Fig. 8(c) shows the XPS wide-scan spectrum of PEG_{173}–PS_{50}–PEG_{173}. The dramatic increase in O 1s peak at 529 eV is consistent with the preparation of PEG_{173}–PS_{50}–PEG_{173}. Fig. 8(d) shows the N 1s core-level spectrum of PEG_{173}–PS_{50}–PEG_{173}. The disappearance peak signal at 403.8 eV assigned to $N^- = N^+ = N$ and the presence of signal at 399.4 eV, 399.8 eV and 400.2 eV with an area ratio of 1.1 : 1.03 : 1.0, is consistent with the formation of 1,2,3-triazole moieties, indicating that the CuAAC reaction has been successfully carried out. Fig. 9 shows the GPC trace of the PEG_{173}–PS_{50}–PEG_{173}, $(PEG_{173})_2$–PS_{50}–$(PEG_{173})_2$ and $(PEG_{173})_3$–PS_{50}–$(PEG_{173})_3$. The M_n increase from 22.6×10^3 g mol^{-1}, 37.5×10^3 g mol^{-1} and 54.8×10^3 g mol^{-1}, respectively, while the PDI remained around 1.30. The number of PEG blocks in $(PEG_{173})_x$–PS_{50}–$(PEG_{173})_x$ copolymers can be calculated according to the following eqn (3):

$$N_{PEG} = \left(M_{n(PEG)_x-PS_{50}-(PEG)_x} - M_{n(N_3)_x\text{-}PS_{50}\text{-}(N_3)_x}\right)/M_{nPEG} \quad (3)$$

Table 1 shows the numbers of PEG blocks in PEG_{173}–PS_{50}–PEG_{173}, $(PEG_{173})_2$–PS_{50}–$(PEG_{173})_2$ and $(PEG_{173})_3$–PS_{50}–$(PEG_{173})_3$ is 2.3, 4.2 and 6.3, respectively, which are comparable to the numbers of bromo groups in the corresponding $(Br)_x$–PS_{50}–$(Br)_x$, and those of azide groups in the corresponding $(N_3)_x$–PS_{50}–$(N_3)_x$ polymers.

Synthesis of APCNs by CuAAC

Well-defined amphiphilic polymer co-networks (APCN) of PS and PEG were prepared from CuAAC of di-alkynyl terminated PEG with M_n of 2000 (PEG_{45}) and $(N_3)_x$–PS_{50}–$(N_3)_x$ ($x = 2, 3$). One of the most attractive features of APCNs is their various physical properties in different solvents due to the existence of both hydrophilic and hydrophobic phases in polymer networks. Scheme 2 illustrates the behavior of the APCNs in various mediums *via* morphological isomerization. In a good solvent for both the hydrophilic and hydrophobic, the polymer chains in the network are highly extended, while in a selective solvent

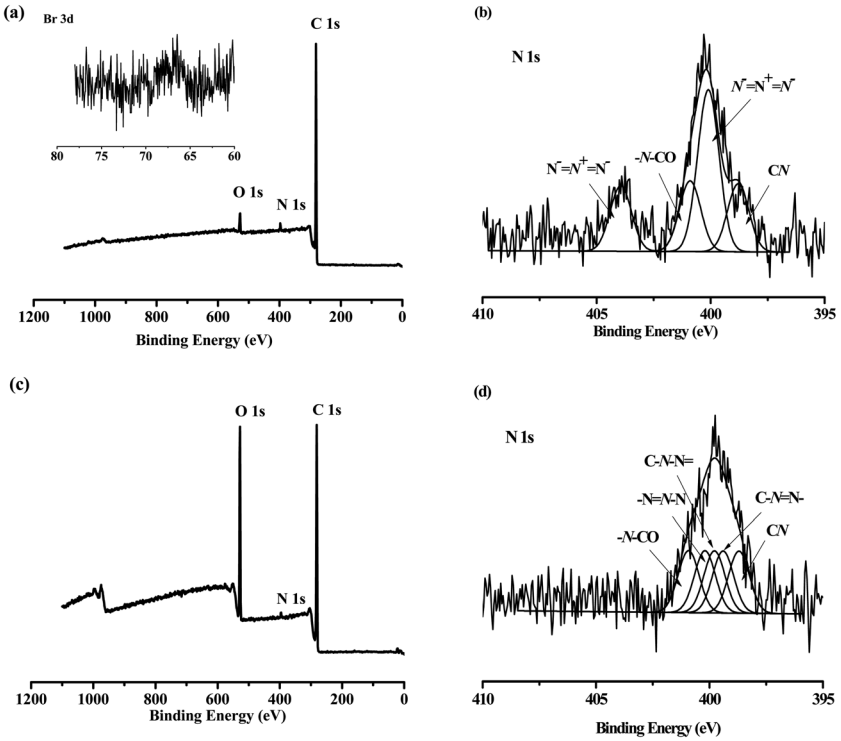

Fig. 8 X-ray photoelectron spectra (XPS) wide-scan spectra of (a) N_3–PS_{50}–N_3 and (c) PEG_{173}–PS_{50}–PEG_{173}. XPS N1s core-level spectra of (b) N_3–PS_{50}–N_3 and (d) PEG_{173}–PS_{50}–PEG_{173}.

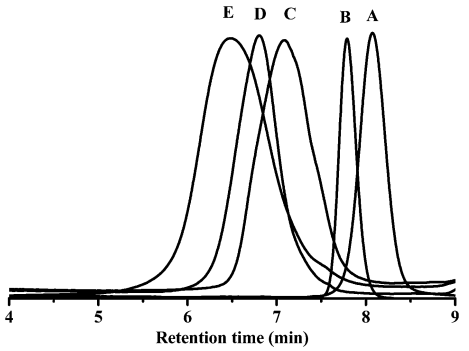

Fig. 9 Gel Permeation Chromatography (GPC) curves of (A) PS_{50} CTA, (B) mono-alkynyl terminated PEG_{173}, (C) PEG_{173}–PS_{50}–PEG_{173}, (D) $(PEG_{173})_2$–PS_{50}–$(PEG_{173})_2$, (E) $(PEG_{173})_3$–PS_{50}–$(PEG_{173})_3$ (eluent: tetrahydrofuran (THF), 40 °C, PS standards).

for either hydrophilic or hydrophobic, only the corresponding part of polymer chains adopts extension. The characteristics result in interesting swelling properties and unique physical properties. Tetrahydrofuran (THF) is a good solvent for both PEG and PS, in which APCNs can fully swell. Fig. 10 shows that all samples swelled and reached equilibration in 150 min. APCN from $(N_3)_3$–PS_{50}–$(N_3)_3$ ($APCN_{PS_{50}\text{-}(PEG45)_3}$) has a maximum swelling ratio (SR) of 470%, which is smaller than that (590%) of APCN from $(N_3)_2$–PS_{50}–$(N_3)_2$ ($APCN_{PS_{50}\text{-}(PEG45)_2}$). The swelling degrees fully agreed with the fact that the more crosslink points, the smaller extension capabilities of the polymer network lattice. Fig. 10 also shows the SR of $APCN_{PS_{50}\text{-}(PEG45)_3}$ and

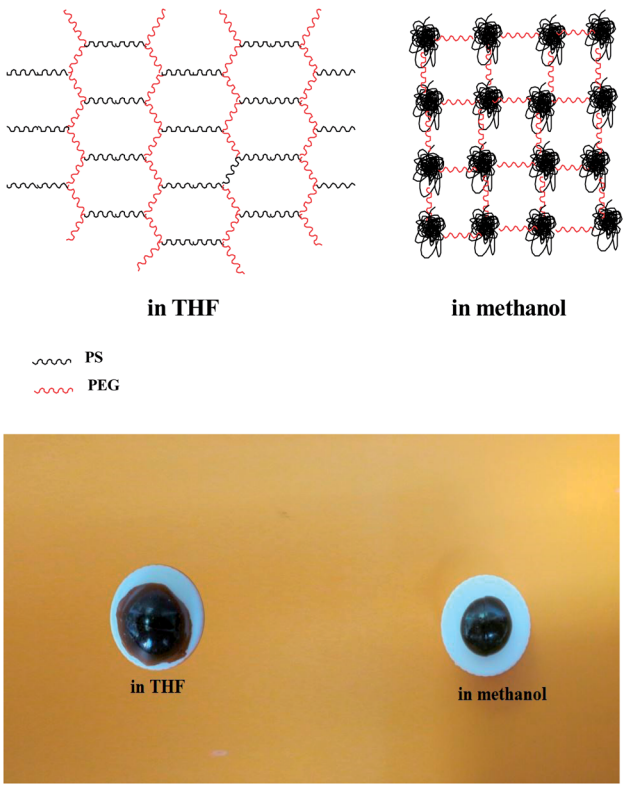

Scheme 2 Schematic illustration of the theoretical swelling behavior and photograph of amphiphilic co-networks (APCNs) in tetrahydrofuran (THF) and methanol.

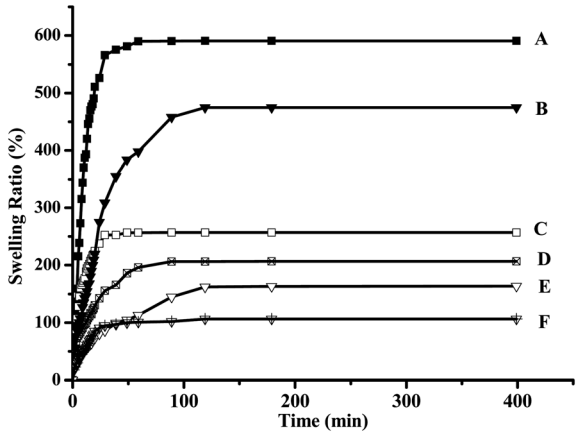

Fig. 10 The swelling ratios of $APCN_{PS_{50}\text{-}(PEG45)_2}$ in (A) tetrahydrofuran (THF), (C) methanol, (D) water and $APCN_{PS_{50}\text{-}(PEG45)_3}$ in (B) THF, (E) methanol, (F) water.

$APCN_{PS_{50}\text{-}(PEG45)_2}$ in methanol and water, respectively, which are good solvent for PEG, but poor for PS. The SR of $APCN_{PS_{50}\text{-}(PEG45)_2}$ are 260% in methanol and 200% in water. The lower of SR of $APCN_{PS_{50}\text{-}(PEG45)_2}$ in water than methanol may account for the higher polarity of former ($\delta = 10.2$) than the later ($\delta = 6.6$). For $APCN_{PS_{50}\text{-}(PEG45)_3}$, the SR are 170% in methanol and 102% in water, respectively. In comparison with SR in THF, all APCNs show a reduced value, which is consistent with the fact that only the PEG segments can extend in methanol or water. The theoretical maximum SR of APCNs in methanol can be calculated based on (4):[52]

$$SR_{maximum} = (L_{PEG}/(L_{PEG}+L_{PS}))^3 \times SR_{THF} \quad (4)$$

The theoretical SR values of $APCN_{PS_{50}\text{-}(PEG45)_2}$ and $APCN_{PS_{50}\text{-}(PEG45)_3}$ are 320% and 240%, respectively, and comparable to experimental value (260% and 170%). This result indicates that the APCNs have well-defined molecular structures.

The thermal stability is very important for materials aiming for biomedical applications. Here, the thermal properties of $APCN_{PS_{50}\text{-}(PEG45)_2}$ and $APCN_{PS_{50}\text{-}(PEG45)_3}$ were studied by thermal gravimetric analysis (TGA) and differential scanning calorimetry (DSC). Fig. 11 shows the TGA curves of dried $APCN_{PS_{50}\text{-}(PEG45)_2}$ and $APCN_{PS_{50}\text{-}(PEG45)_3}$. APCNs undergo one-step weight loss behavior, which occurs at about 237 °C. The one step decomposition behavior reveals that PS and PEG well distribute in molecular level, which is consisted with the well-defined

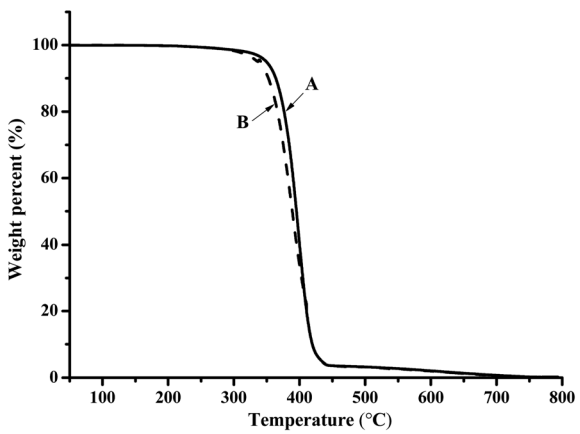

Fig. 11 Thermogravimetric analysis (TGA) curves of (A) $APCN_{PS_{50}\text{-}(PEG45)_2}$ and (B) $APCN_{PS_{50}\text{-}(PEG45)_3}$.

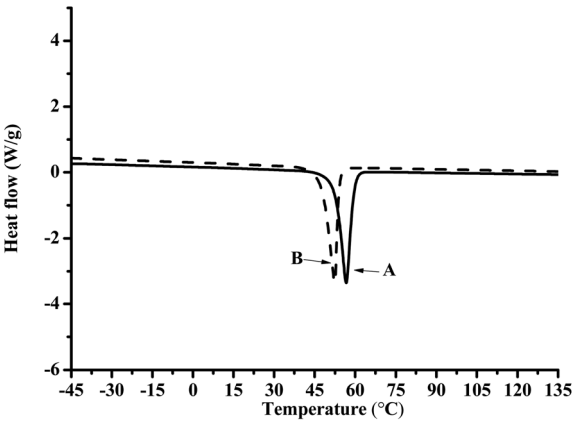

Fig. 12 Differential scanning calorimetry (DSC) curves of (A) $APCN_{PS_{50}\text{-}(PEG45)_2}$ and (B) $APCN_{PS_{50}\text{-}(PEG45)_3}$.

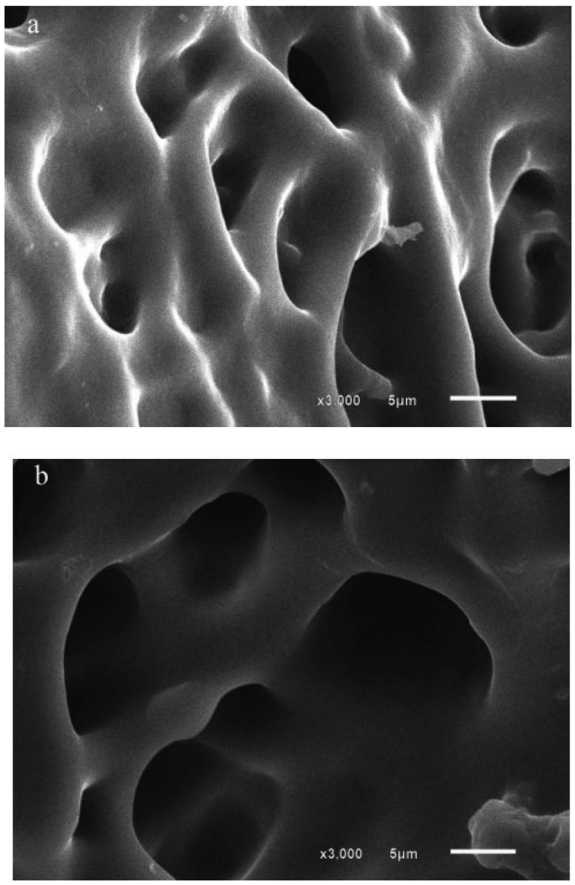

Fig. 13 Scanning electron microscopy (SEM) cross-sectional views of the freeze-dried samples of (a) $APCN_{PS_{50}\text{-}(PEG45)_3}$ and (b) $APCN_{PS_{50}\text{-}(PEG45)_2}$.

molecular structure of the APCNs. Fig. 12 also shows the DSC results of $APCN_{PS_{50}\text{-}(PEG45)_2}$ and $APCN_{PS_{50}\text{-}(PEG45)_3}$. The melting behavior of the APCNs is largely affected by the content of PEG and PS blocks. There are one endothermic at 56.7 °C in the heating process, assigned to T_m of PEG segments in $APCN_{PS_{50}\text{-}(PEG45)_2}$. While for $APCN_{PS_{50}\text{-}(PEG45)_3}$, T_m shifts to 52.1 °C due to the increase of the PEG content. No endothermic peak for the T_g of the PS segments was detected, because of a relatively short chain length and uniform distribution of PS in APCN. The morphology of APCN was further investigated by scanning electron microscopy (SEM). Fig. 13 shows the SEM cross section view of freeze-dried $APCN_{PS_{50}\text{-}(PEG45)_3}$ and $APCN_{PS_{50}\text{-}(PEG45)_2}$. The $APCN_{PS_{50}\text{-}(PEG45)_3}$ show a denser pores than that of $APCN_{PS_{50}\text{-}(PEG45)_2}$, which is consistent with the higher density of crosslink point and high concentration polymer chains in $APCN_{PS_{50}\text{-}(PEG45)_3}$.

Conclusions

In summary, we have developed a robust approach to control the number of end groups in linear polymers by multiple alternating RAFT polymerization of electron-deficient and electron-rich monomers. PS with exactly 2, 4 and 6 bromo or azide groups at chain ends were successfully prepared *via* multiple step alternating RAFT chain extension of Pin and PBMI. Well-defined copolymer $(PEG)_x$–PS_{50}–$(PEG)_x$ and $APCN_{PS_{50}\text{-}(PEG45)_x}$ $(x = 2, 3)$ were successfully obtained *via* CuAAC of the $(N_3)_x$–PS_{50}–$(N_3)_x$ $(x = 2, 3)$ polymer with mono-alynyl and di-alkynyl terminated PEG. $APCN_{PS_{50}\text{-}(PEG45)_2}$ and $APCN_{PS_{50}\text{-}(PEG45)_3}$ exhibit a well-defined molecular structure and various SR in different solvents. The SR of co-polymer network can be regulated by the control of size and composition of the pre-macromolecule due to the well-defined molecular structure of polymer network. The precise synthesis of linear polymers with named number of functional groups on ends provides a novel strategy for the preparation of well-defined copolymers and polymer network with tailored molecular structure, good structural integrity and desired functionalities.

Conflict of interest

The authors declare no competing financial interest.

Acknowledgements

This work was supported by National Natural Science Foundation of China (no. 21074022, no. 21274020 and no. 21304019) and Jiangsu Key Laboratory of Advanced Functional Polymer Design and Application (no. KJS1138, Soochow University).

References

1 N. A. Peppas, J. Z. Hilt, A. Khademhosseini and R. Langer, *Adv. Mater.*, 2006, **18**(11), 1345–1360.
2 F. Brandl, F. Sommer and A. Goepferich, *Biomaterials*, 2007, **28**(2), 134–146.
3 G. Erdodi and J. P. Kennedy, *Prog. Polym. Sci.*, 2006, **31**(1), 1–18.
4 L. Mespouille, J. L. Hedrick and P. Dubois, *Soft Matter*, 2009, **5**(24), 4878–4892.
5 C. S. Patrickios and T. K. Georgiou, *Curr. Opin. Colloid Interface Sci.*, 2003, **8**(1), 76–85.
6 D. Kafouris, M. Gradzielski and C. S. Patrickios, *Macromolecules*, 2009, **42**(8), 2972–2980.
7 T. K. Georgiou, M. Vamvakaki and C. S. Patrickios, *Polymer*, 2004, **45**(21), 7341–7355.
8 M. Vamvakaki and C. S. Patrickios, *J. Phys. Chem. B*, 2001, **105**(21), 4979–4986.
9 J. Künzler and R. Ozark, *J. Appl. Polym. Sci.*, 1997, **65**(6), 1081–1089.
10 J. Xu, X. Li and F. Sun, *Drug Delivery*, 2011, **18**(2), 150–158.
11 P. C. Nicolson and J. Vogt, *Biomaterials*, 2001, **22**(24), 3273–3283.
12 E. Behravesh, S. Jo, K. Zygourakis and A. G. Mikos, *Biomacromolecules*, 2002, **3**(2), 374–381.
13 R. Haigh, N. Fullwood and S. Rimmer, *Biomaterials*, 2002, **23**(16), 3509–3516.
14 R. Haigh, S. Rimmer and N. J. Fullwood, *Biomaterials*, 2000, **21**(7), 735–739.
15 Y. Sun, J. Collett, N. J. Fullwood, S. Mac Neil and S. Rimmer, *Biomaterials*, 2007, **28**(4), 661–670.
16 S. Rimmer, M. J. German, J. Maughan, Y. Sun, N. Fullwood, J. Ebdon and S. MacNeil, *Biomaterials*, 2005, **26**(15), 2219–2230.
17 D. F. E. Prez, E. J. Goethals, R. Schué, H. Qariouh and F. Schué, *Polym. Int.*, 1998, **46**(2), 117–125.
18 W. Reyntjens, L. Jonckheere, E. Goethals and F. Du Prez, *Macromol. Symp.*, 2001, **164**, 293–300.
19 N. Bruns and J. C. Tiller, *Nano Lett.*, 2005, **5**(1), 45–48.
20 G. Savin, N. Bruns, Y. Thomann and J. C. Tiller, *Macromolecules*, 2005, **38**(18), 7536–7539.
21 N. Bruns, W. Bannwarth and J. C. Tiller, *Biotechnol. Bioeng.*, 2008, **101**(1), 19–26.
22 E. M. Hensle, J. Tobis, J. C. Tiller and W. Bannwarth, *J. Fluorine Chem.*, 2008, **129**(10), 968–973.
23 L. Bromberg, M. Temchenko and T. A. Hatton, *Langmuir*, 2002, **18**(12), 4944–4952.
24 C. Lin and I. Gitsov, *Macromolecules*, 2010, **43**(23), 10017–10030.
25 J. P. Kennedy, *Macromol. Symp.*, 2001, **175**, 127–131.
26 J. P. Kennedy, G. Fenyvesi, S. Na, B. Keszler and K. S. Rosenthal, Amphiphilic gels with controlled mesh dimensions for insulin delivery, in *Polymer Gels: Fundamentals and Applications*, ed. H. B. Bohidar, P. Dubin and Y. Osada, Amer Chemical Soc, Washington, 2003, vol. 833, pp. 290–299.
27 K. Podual, F. Doyle,III and N. Peppas, *Polymer*, 2000, **41**(11), 3975–3983.
28 E. Themistou and C. S. Patrickios, *Macromolecules*, 2004, **37**(18), 6734–6743.
29 E. Loizou, A. I. Triftaridou, T. K. Georgiou, M. Vamvakaki and C. S. Patrickios, *Biomacromolecules*, 2003, **4**(5), 1150–1160.

30 M. R. Simmons, E. N. Yamasaki and C. S. Patrickios, *Macromolecules*, 2000, **33**(8), 3176–3179.
31 N. Simha, C. Carlson and J. Lewis, *J. Mater. Sci.: Mater. Med.*, 2004, **15**(5), 631–639.
32 J. P. Gong, *Soft Matter*, 2010, **6**(12), 2583–2590.
33 M. Delerba, J. R. Ebdon and S. Rimmer, *Macromol. Rapid Commun.*, 1997, **18**(8), 723–728.
34 D. L. Elbert, A. B. Pratt, M. P. Lutolf, S. Halstenberg and J. A. Hubbell, *J. Controlled Release*, 2001, **76**(1), 11–25.
35 F. Cellesi, N. Tirelli and J. A. Hubbell, *Biomaterials*, 2004, **25**(21), 5115–5124.
36 S. C. Rizzi and J. A. Hubbell, *Biomacromolecules*, 2005, **6**(3), 1226–1238.
37 B. H. Lee, B. West, R. McLemore, C. Pauken and B. L. Vernon, *Biomacromolecules*, 2006, **7**(6), 2059–2064.
38 R. Riva, S. Schmeits, F. Stoffelbach, C. Jerome, R. Jerome and P. Lecomte, *Chem. Commun.*, 2005, 5334–5336.
39 R. Riva, S. Schmeits, C. Jérôme, R. Jérôme and P. Lecomte, *Macromolecules*, 2007, **40**(4), 796–803.
40 G. Mantovani, V. Ladmiral, L. Tao and D. M. Haddleton, *Chem. Commun.*, 2005, 2089–2091.
41 J. A. Opsteen and J. C. M. van Hest, *Chem. Commun.*, 2005, 57–59.
42 M. van Dijk, D. T. S. Rijkers, R. M. J. Liskamp, C. F. van Nostrum and W. E. Hennink, *Bioconjugate Chem.*, 2009, **20**(11), 2001–2016.
43 M. Malkoch, R. Vestberg, N. Gupta, L. Mespouille, P. Dubois, A. F. Mason, J. L. Hedrick, Q. Liao, C. W. Frank, K. Kingsbury and C. J. Hawker, *Chem. Commun.*, 2006, 2774–2776.
44 V. Crescenzi, L. Cornelio, C. Di Meo, S. Nardecchia and R. Lamanna, *Biomacromolecules*, 2007, **8**(6), 1844–1850.
45 D. A. Ossipov and J. Hilborn, *Macromolecules*, 2006, **39**(5), 1709–1718.
46 J. A. Johnson, D. R. Lewis, D. D. Díaz, M. G. Finn, J. T. Koberstein and N. J. Turro, *J. Am. Chem. Soc.*, 2006, **128**(20), 6564–6565.
47 J. A. Johnson, M. G. Finn, J. T. Koberstein and N. J. Turro, *Macromolecules*, 2007, **40**(10), 3589–3598.
48 J. A. Johnson, J. M. Baskin, C. R. Bertozzi, J. T. Koberstein and N. J. Turro, *Chem. Commun.*, 2008, 3064–3066.
49 J. A. Johnson, M. Finn, J. T. Koberstein and N. J. Turro, *Macromol. Rapid Commun.*, 2008, **29**(12-13), 1052–1072.
50 J. Zednik, R. Riva, P. Lussis, C. Jérôme, R. Jérôme and P. Lecomte, *Polymer*, 2008, **49**(3), 697–702.
51 V. Truong, I. Blakey and A. K. Whittaker, *Biomacromolecules*, 2012, **13**(12), 4012–4021.
52 Y. Yuan, A.-K. Zhang, J. Ling, L.-H. Yin, Y. Chen and G.-D. Fu, *Soft Matter*, 2013, **9**, 6309–6318.
53 G. Hild, *Prog. Polym. Sci.*, 1998, **23**(6), 1019–1149.
54 J.-S. Wang and K. Matyjaszewski, *Macromolecules*, 1995, **28**(23), 7901–7910.
55 R. áO'Dell and S. áP Armes, *Chem. Commun.*, 1999, 1285–1286.
56 K. Matyjaszewski and J. Xia, *Chem. Rev.*, 2001, **101**(9), 2921–2990.
57 Q. Yu, F. Zeng and S. Zhu, *Macromolecules*, 2001, **34**(6), 1612–1618.
58 Q. Liu, P. Zhang, A. Qing, Y. Lan and M. Lu, *Polymer*, 2006, **47**(7), 2330–2336.
59 M. Achilleos, T. M. Legge, S. Perrier and C. S. Patrickios, *J. Polym. Sci., Part A: Polym. Chem.*, 2008, **46**(22), 7556–7565.
60 H. Willcock and R. K. O'Reilly, *Polym. Chem.*, 2010, **1**(2), 149–157.
61 H. Li, B. Yu, H. Matsushima, C. E. Hoyle and A. B. Lowe, *Macromolecules*, 2009, **42**(17), 6537–6542.
62 G. Gody, C. Rossner, J. Moraes, P. Vana, T. Maschmeyer and S. b. Perrier, *J. Am. Chem. Soc.*, 2012, **134**(30), 12596–12603.
63 J. Maślińska-Solich and I. Rudnicka, *Eur. Polym. J.*, 1988, **24**(5), 453–456.
64 F. Cataldo, M. Gobbino, O. Ursini and G. Angelini, *J. Macromol. Sci., Part A: Pure Appl. Chem.*, 2007, **44**(11), 1225–1234.
65 Y. Wang, Q. Chen, H. Liang and J. Lu, *Polym. Int.*, 2007, **56**(12), 1514–1520.
66 L. M. Salonen, C. Bucher, D. W. Banner, W. Haap, J. L. Mary, J. Benz, O. Kuster, P. Seiler, W. B. Schweizer and F. Diederich, *Angew. Chem., Int. Ed.*, 2008, **48**(4), 811–814.
67 A. M. Eissa and E. Khosravi, *Eur. Polym. J.*, 2011, **47**(1), 61–69.
68 L. QunáXu and G. DongáFu, *Polym. Chem.*, 2012, **3**(4), 920–927.
69 B. Mrabet, A. Mejbri, S. Mahouche, S. Gam-Derouich, M. Turmine, M. Mechouet, P. Lang, H. Bakala, M. Ladjimi and A. Bakhrouf, *Surf. Interface Anal.*, 2011, **43**(11), 1436–1443.
70 J. Lu, H. Liang, W. Zhang and Q. Cheng, *J. Polym. Sci., Part A: Polym. Chem.*, 2003, **41**(9), 1237–1242.
71 C. R. Nair, *Macromolecules*, 1993, **26**(1), 47–54.
72 A.-L. Li, W. Zhang, H. Liang and J. Lu, *Polymer*, 2004, **45**(19), 6533–6537.
73 M. Buback, O. Janssen, R. Oswald, S. Schmatz and P. Vana, in A Missing Reaction Step in Dithiobenzoate – Mediated RAFT Polymerization, *Macromol. Symp*, 2007, Wiley Online Library, pp. 158–167.
74 G. Moad, E. Rizzardo and S. H. Thang, *Aust. J. Chem.*, 2005, **58**(6), 379–410.
75 A. Feldermann, M. L. Coote, M. H. Stenzel, T. P. Davis and C. Barner-Kowollik, *J. Am. Chem. Soc.*, 2004, **126**(48), 15915–15923.
76 S. Lee, B. Lee, B. J. Kim, J. Park, M. Yoo, W. K. Bae, K. Char, C. J. Hawker, J. Bang and J. Cho, *J. Am. Chem. Soc.*, 2009, **131**(7), 2579–2587.
77 R. K. O'Reilly, M. J. Joralemon, C. J. Hawker and K. L. Wooley, *J. Polym. Sci., Part A: Polym. Chem.*, 2006, **44**(17), 5203–5217.
78 J. P. Collman, N. K. Devaraj, T. P. Eberspacher and C. E. Chidsey, *Langmuir*, 2006, **22**(6), 2457–2464.

